ELSEVIER

Contents lists available at ScienceDirect

Journal of Molecular Spectroscopy

journal homepage: www.elsevier.com/locate/yjmsp





Parent, ³⁴S, and deuterated triflic acid: Microwave spectra and tunneling splittings due to hydroxyl torsion

Anna K. Huff, Nathan Love, C.J. Smith, Kenneth R. Leopold *

Department of Chemistry, University of Minnesota, 207 Pleasant St. SE, Minneapolis, MN 55455, United States

ARTICLE INFO

Keywords:
Triflic acid
Microwave spectroscopy
Tunneling splitting
Hydroxyl torsional motion
Selection rules
Chirped-pulse and cavity microwave

ABSTRACT

Spectra for the parent, ³⁴S, and deuterated forms of triflic acid (CF₃SO₃H) have been observed by chirped-pulse and cavity Fourier transform microwave spectroscopy. The observation of a-, b-, and c-type transitions definitively establishes that the molecule does not have C_s symmetry, and M06-2X/6-311++G(3df,3pd) calculations concur, yielding a structure in which the OH bond is nearly perpendicular to the C-S-O(H) plane. The rotational spectrum for each isotopologue exhibits a pair of tunneling states resulting from large amplitude motion of the hydroxyl hydrogen between two equivalent structures with opposite directions of the OH bond. The experimentally determined tunneling energies, ΔE , for the parent and 34 S species are 52.96784(65) MHz and 52.8761(16) MHz, respectively. For the -OD isotopologue, the tunneling energy decreases significantly, with a value of only $\Delta E = 0.2460(20)$ MHz. Curiously, we observe that b-type transitions cross between tunneling states in the parent and ^{34}S spectra, while c-type transitions cross in the spectra of the deuterated species. This likely arises because the molecule is close to a symmetric top, with only the location of the hydrogen defining the orientation of the b- and c-inertial axes, enabling slight structural changes to switch the axis orientations at the $transition \ state. \ Calculations \ at \ the \ M06-2X/6-311++G(3df,3pd) \ level \ of \ theory \ predict \ a \ 2.8 \ kcal/mol \ barrier$ for the large amplitude motion of the hydroxyl hydrogen rotating around the S-O bond through a C_s symmetric transition state in which the O-H is oriented anti with respect to the S-C bond. A complete scan of the hydroxyl proton around the S-O bond shows an additional transition state of C_s symmetry in the syn orientation with a 6.2 kcal/mol barrier relative to the equilibrium configuration.

1. Introduction

Since their advent in the mid-20th century, the use of superacids has become widespread in chemistry [1]. Relative to other strong acids and superacids, triflic acid is particularly useful in many synthetic applications because it is non-oxidizing, stable at high temperatures, and forms a conjugate base that is only weakly nucleophilic [2,3]. The properties of triflic acid have also been exploited in the form of a key functional group in the application of proton exchange membrane fuel cells which have been studied extensively by computational and experimental methods [4_10]

Triflic acid itself has been previously studied by various experimental techniques. The gas-phase structure was determined from electron diffraction in 1981 [11] and the vibrational spectra in the gaseous, liquid, and solid phases have been reported [12–14]. The vapor phase -OH overtone spectrum has also been observed by cavity ring-down spectroscopy [15].

Complexes of triflic acid also serve as excellent venues for studying proton transfer in the gas phase. Because of its superacidity, its complexes with bases such as water and amines offer the opportunity to observe ion pair formation in species small enough to be studied by rotational spectroscopy. For example, the complex formed from trimethylamine and triflic acid has recently been reported [16] and shown to be best described as a trimethylammonium triflate ion pair, even without the stabilization afforded by microsolvation. In contrast, a study of the first three hydrates of the acid, CF_3SO_3H - $(H_2O)_{n=1-3}$, has demonstrated that three water molecules are required for proton transfer [17]. In this work we report the microwave spectrum of the triflic acid monomer, as well as its ³⁴S and deuterated isotopologues. Tunneling states arising from hydroxyl torsion are observed and in each case the energy separation between these states has been experimentally determined. Computational work is also reported which investigates the tunneling path and the barrier to the hydroxyl large amplitude motion.

E-mail address: kleopold@umn.edu (K.R. Leopold).

^{*} Corresponding author.

2. Computational methods and results

The minimum energy structure of triflic acid was optimized at the M06-2X/6-311++G(3df,3pd) level of theory using the Gaussian16 suite of programs [18] and is shown in Fig. 1. Following the atom labeling in the figure, the predicted structure shows the hydroxyl group oriented roughly along the S1=O9 bond with a O9-S1-O2-H3 dihedral angle of 19.1 deg. However an energetically equivalent structure with identical rotational constants can be obtained when the hydroxyl group is instead oriented along the S1=O8 bond. A rotation of OH around the S1-O2 bond would allow the interconversion between the two structures. Several levels of theory, including MP2/aug-cc-pVDZ, B2PLYP-D3BJ/ jun-cc-pVTZ, and DSD-PBEP86-D3BJ/jun-cc-pVTZ, were also tested and concur with these results. With these methods, the basis sets aug-cc-pV (n + d)Z and jun-cc-pV(n + d)Z (n = T, D) were obtained from the Basis Set Exchange library and used on the sulfur atom to include an additional set of tight d functions [19]. The corresponding calculated dihedral angles and barriers are provided in the Supplementary Material.

To further explore the hydroxyl proton tunneling path, a computational scan of the C4-S1-O2-H3 dihedral angle in 2 degree increments was carried out at the M06-2X/6-311++G(3df,3pd) level with the result shown in Fig. 2. The dihedral angles at the minimum energy structures are 92.3 degrees and 267.7 degrees, and two barriers separate the equivalent minima depending on whether the hydroxyl proton rotates away from (180 degrees) or towards the CF3 group (0/360 degrees). Using the energies from the optimized C_s symmetric transition state geometries, a barrier of 2.8 kcal/mol (2.2 kcal/mol with zero-point corrections) is calculated when the hydroxyl proton rotates around the S1-O2 bond to pass through the transition state where the hydroxyl group is oriented *anti* with respect to the S-C bond. When the hydroxyl proton instead rotates through the *syn* transition state structure, the height of the barrier is 6.2 kcal/mol (5.6 kcal/mol with zero-point corrections).

3. Experimental methods and results

Rotational spectra of triflic acid were collected using a tandem cavity and chirped-pulse Fourier transform microwave spectrometer, details of which have been given elsewhere [20,21]. Estimated uncertainties for the cavity measurements are about 3 kHz, while those obtained on the chirped-pulse system are about 10 kHz. Argon was pulsed through the 0.8 mm orifice of a stainless steel cone nozzle at a stagnation pressure of 1.3 atm. Triflic acid vapor was introduced separately by flowing 0.5 atm of argon through a reservoir of liquid triflic acid (Sigma Aldrich, 99%) and injecting the vapor into the expansion about 5 mm downstream from the nozzle orifice through a 0.016 in. inner diameter hypodermic needle as described previously [22]. The ³⁴S species was observed in natural abundance and a sample of isotopically enriched deuterated triflic acid (CF₃SO₃D, Sigma Aldrich, 98%) was used to collect spectra

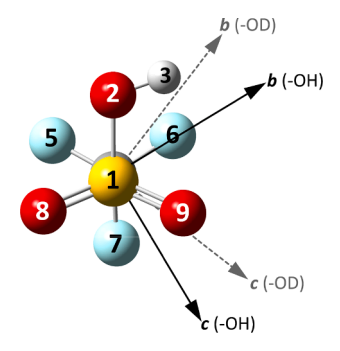


Fig. 1. M06-2X/6-311++G(3df,3pd) minimum energy structure of triflic acid. The principal axis system orientations for the -OH and -OD isotopologues are shown with solid black and dashed grey axes, respectively.

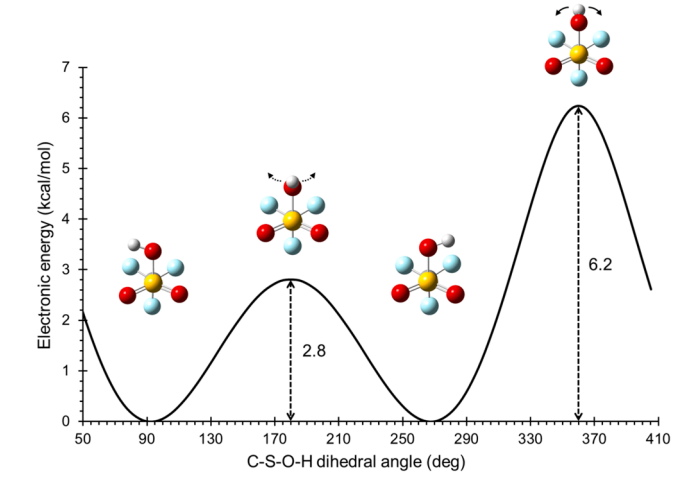


Fig. 2. A scan of potential energy as a function of the C-S-O-H dihedral angle performed at the M06-2X/6-311++G(3df,3pd) level of theory. A 2.8 kcal/mol barrier separates the equivalent minima when going through a transition state geometry with a dihedral angle of 180 deg (hydroxyl oriented *anti* with respect to the S-C bond). A 6.2 kcal/mol barrier separates the minima when going through a transition state geometry at a 360 deg dihedral angle (hydroxyl oriented *syn* with respect to the S-C bond). Structures shown with arrows indicate the transition state geometries and their respective imaginary frequencies. Dotted arrows indicate the OH unit swinging back. Solid arrows indicate it swinging forward.

for the deuterated isotopologue. Because of its low vapor pressure as well as its corrosivity, the reservoir of liquid triflic acid was located only a few inches upstream from the injection needle to minimize the traveling distance through the gas lines to the vacuum chamber.

Parent and ³⁴S Triflic Acid: A 6–18 GHz chirped-pulse spectrum of triflic acid was collected in 3 GHz segments, each averaged between 170,000 and 900,000 free induction decay (FID) signals, with each FID collected for 20 µs. The full spectrum is shown in Fig. 3. Dipole moment components for the predicted structure occur along each of the inertial axes, with the b-type spectrum expected to be the most intense $(|\mu_a| = 0.5 \text{ D}, |\mu_b| = 2.5 \text{ D}, |\mu_c| = 1.3 \text{ D})$. All three transition types were observed and each revealed the presence of a pair of tunneling states (designated 0⁺ and 0⁻ for the ground and excited states, respectively), presumably due to large amplitude motion of the hydroxyl group across either side of the C_s symmetric transition state. The α - and c-type transitions appeared as closely spaced pairs and were assigned as occurring within the same tunneling state. The pairs of b-type transitions were assigned as crossing between tunneling states $(0^{\mp} \leftarrow 0^{\pm})$ and were separated by 106–154 MHz with increasing *J* from J'' = 0 up to J'' = 6. (The variation with increasing J is due to rotation-vibration interactions described below.) The separation of 106 MHz for the $1_{11} \leftarrow 0_{00}$ transition is approximately twice the value of ΔE . Note that these assignments were aided by closed loops and attempts to assign the cross-state transitions as c-type lines resulted in negative values of (B - C).

All fits were performed using Pickett's SPFIT program [23]. After achieving an initial fit from the chirped-pulse data, pairs of weaker transitions were located using the cavity spectrometer. Additionally, for the a-type spectra, several of the observed ground and excited state pairs were unresolvable at low J for $K_a=0$ and $K_a=2$ but became resolvable on the cavity spectrometer at J''=4, with small splittings on the order of about 20 kHz. In contrast, the $K_a=1$ ground and excited state transitions were separated by about 5 to 80 MHz, increasing with increasing J. Two forbidden transitions (515, 0 $^ \leftarrow$ 413, 0 $^+$ and 514, 0 $^+$ \leftarrow 414, 0 $^-$) were predicted and subsequently observed within a few kHz of their calculated frequencies.

In total, 150 transitions were assigned to 129 distinct frequencies for the parent species between 3 and 18 GHz ranging from J'' = 0 to J'' = 6

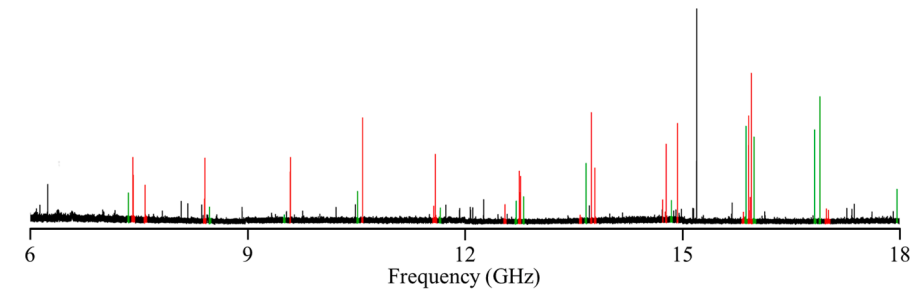


Fig. 3. 6–18 GHz chirped-pulse spectrum of parent triflic acid in argon resulting from the average of 170,000 free induction decay (FID) signals. Each FID was collected for 20 μ s. Instrument artifacts have been removed from the spectrum. The prominent series of lines highlighted in red and green are select *c*-type and *b*-type transitions, respectively, mostly involving $K_a{}^{\prime\prime}=0$ and 1 for the triflic acid monomer. Remaining lines in the spectrum are primarily additional triflic acid monomer transitions with higher values of $K_a{}^{\prime\prime}$.

Table 1Spectroscopic constants from the combined fits of lower and upper states for the parent and ³⁴S isotopologues of triflic acid.^a

	CF ₃ SO ₃ H		CF_3 ³⁴ SO_3H		
	0+	0-	0+	0-	
A [MHz]	2669.06754(18)	2669.06740(17)	2668.69479(39)	2668.69467(25)	
B [MHz]	1586.31446(17)	1586.31459(12)	1578.45686(30)	1578.45556(26)	
C [MHz]	1582.53271(12)	1582.53242(13)	1574.85992(33)	1574.85936(32)	
Δ_J [kHz]	0.1332(26)	0.1373(27)	0.1495(98)	0.124(10)	
Δ_{JK} [kHz]	0.0706(37)	0.0624(42)	[0.0706]	[0.0624]	
Δ_K [kHz]	-0.0609(90)	-0.056(11)	[-0.0609]	[-0.056]	
$ F_{bc} [MHz]^b$	4.016073(67)		3.99266(15)		
ΔE [MHz]	52.96784(65)		52.8761(16)		
N^{c}	150		39		
RMS [kHz]d	3.3		3.1		

- (a) Numbers in parentheses are one standard error in the least squares fit. Numbers in brackets in the $CF_3^{34}SO_3H$ fit were held fixed to the values determined in the parent fit.
- (b) Sign cannot be determined in the fit.
- (c) Number of transitions included in the fit. For the parent, 150 transitions were assigned to 129 distinct frequencies. For the ³⁴S isotopologue, 39 transitions were assigned to 36 frequencies.
- (d) Root-mean square deviation of the residuals.

and up to $K_a{''}=4$ for R-branch transitions and from J''=4 to J''=11 with $K_a{''}=3$ and 4 for Q-branch transitions. Cavity measurements were obtained for 79 of the 129 observed frequencies. In the final fits, both states were treated simultaneously with the following Hamiltonian for the parent and 34 S species

$$H = \sum_{n=0}^{1} \left[H_{rot}^{(n)} + H_{cd}^{(n)} + \delta_{n,1} \Delta E \right] + H_{int}$$
 (1)

Here, H_{rot} and H_{cd} are the rigid rotor and centrifugal distortion Hamiltonians, respectively, n=0 and 1 for the 0^+ and 0^- states, respectively, $\delta_{n,1}$ is the Kronecker delta, and ΔE is the energy separation between the tunneling states. The Watson-A reduced Hamiltonian in the I^r representation [24] was used for the centrifugal distortion terms. (Attempts to employ the S-reduction were also tried and had no effects on the results.) $H_{\rm int}$ is the interaction Hamiltonian coupling the tunneling states and is given by [25]

$$H_{int} = F_{bc}(P_b P_c + P_c P_b) \tag{2}$$

where F_{bc} is the interaction constant. The choice of H_{int} depends on the symmetry of the molecule and of the vibrational motion corresponding to the tunneling. For triflic acid, it is reasonable to assume that the tunneling occurs between the two energy minima separated by the transition states represented in Fig. 2 and that the dominant tunneling path involves the one with the lower barrier, i.e., with the -OH pointed away from the CF₃. Both transition state structures of Fig. 2 belong to the C_S symmetry point group and the tunneling motion belongs to the odd symmetry species, A", because it interconverts the two equivalent minimum energy configurations on opposite sides of the σ_h plane. Accordingly, terms with A" symmetry will connect the O^+ and O^- tunneling states. For the parent and O^+ species, the spectra indicate

that the *b*-coordinate is inverted (because the *b*-type transitions cross between tunneling states) and thus for these isotopologues, rotations about the *a*- and *c*-axes (R_a and R_c) belong to the A" species. In the formulation of the reduced axis system, these give rise to F_{bc} and F_{ab} terms, respectively, but attempts to include the F_{ab} term resulted in highly correlated constants and did not provide a significantly better fit. Therefore, F_{bc} was the only interaction parameter used.

The fitted spectroscopic constants for parent triflic acid are given in Table 1. Note that the sign of F_{bc} cannot be determined since the rotational energies depend on the square of the coupling constant. The sign of the product of F_{bc} · μ_b · μ_c does, however, affect the simulated relative intensities of the lower and upper state transitions [26–29]. An example of the observed and calculated relative intensities is shown for the $4_{22} \leftarrow 3_{12}$ and $4_{23} \leftarrow 3_{13}$ transitions in Fig. 4. As seen in the figure, approximate relative intensities of the 0^+ and 0^- transitions are more accurately simulated when the sign of F_{bc} : μ_b : μ_c is positive.

Interestingly, although the separation between ground and excited state pairs generally increases with J across the different spectral types, a noticeable deviation from the trend occurs with the c-type $5_{14} \leftarrow 4_{04}$ and b-type $5_{15} \leftarrow 4_{04}$ lines. The ground state transitions of the $(J''+1)_{1,J''} \leftarrow J''_{0,J''}$ series (of which $5_{14} \leftarrow 4_{04}$ is the J''=4 member) are located 5, 20, and 48 MHz below their respective excited state partner for J''=1 through J''=3. For J''=4, however, the ground state transition is 32 MHz above its excited state analogue. In the case of the b-type $(J''+1)_{1,J''+1} \leftarrow J''_{0,J''}$ series, the $0^- \leftarrow 0^+$ transitions are 111, 126, and 154 MHz above their respective $0^+ \leftarrow 0^-$ partner for J''=1 through J''=3, but the $5_{15} \leftarrow 4_{04}$ $0^- \leftarrow 0^+$ is only 74 MHz above the $5_{15} \leftarrow 4_{04}$ $0^+ \leftarrow 0^-$. This suggests a level crossing in the vicinity of J=4-6, $K_a=1$. An energy level diagram constructed from the energies determined both with and without coupling is shown in Fig. 5 and clearly displays the near-resonances. Specifically, when the perturbations are not treated, it

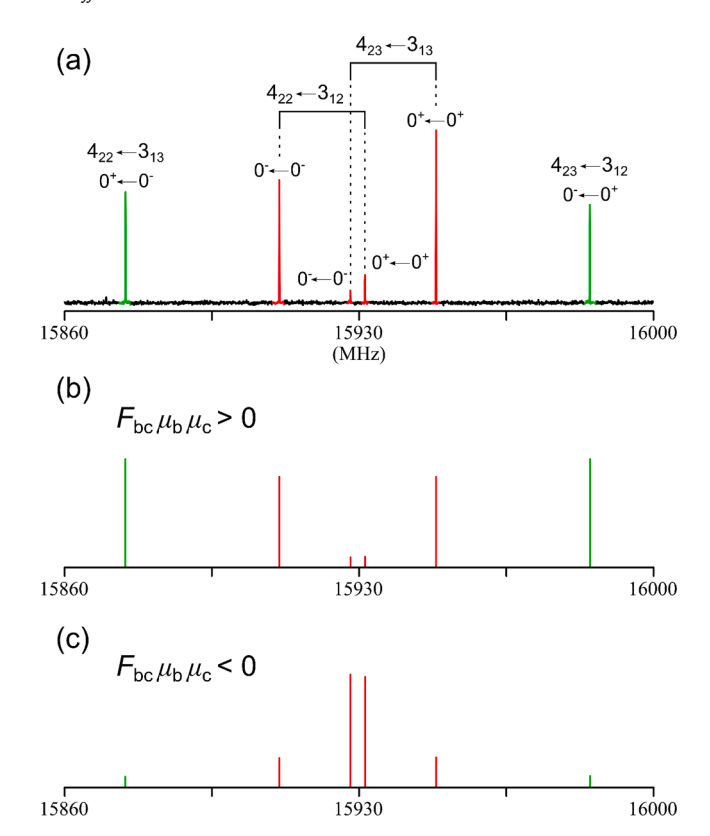


Fig. 4. (a) Excerpt of the chirped-pulse spectrum of triflic acid in argon from 15,860-16,000 MHz showing the $4_{22}\leftarrow 3_{12}$ and $4_{23}\leftarrow 3_{13}$ ground and excited state transitions. Also shown are the $4_{22}\leftarrow 3_{13}$ $0^+\leftarrow 0^-$ and $4_{23}\leftarrow 3_{12}$ $0^-\leftarrow 0^+$ transitions whose counterparts are displaced outside the given excerpt. (b) Simulated spectrum using the fitted CF₃SO₃H rotational constants where the sign of the product of $F_{bc}\cdot\mu_b\cdot\mu_c$ is positive. (c) Simulated spectrum using the fitted CF₃SO₃H rotational constants where the sign of the product of $F_{bc}\cdot\mu_b\cdot\mu_c$ is negative.

can be seen that a level crossing occurs at 5_{14} , $0^+/5_{15}$, 0^- and that these rotational states are separated by only about 4 MHz. The effect of the perturbation also manifested as a sudden change in relative intensities of the b- and c-type transitions near 17 GHz where the b-type $5_{15} \leftarrow 4_{04}$, $0^+ \leftarrow 0^-$ and $5_{15} \leftarrow 4_{04}$, $0^- \leftarrow 0^+$ transitions appear to be borrowing

intensity from the nearby c-type $5_{14} \leftarrow 4_{04}$, $0^- \leftarrow 0^-$ and $5_{14} \leftarrow 4_{04}$, $0^+ \leftarrow 0^+$ lines.

Further indication of strong mixing is obtained from values of the parameter $(1-P_{\rm mix})$, which is produced by Pickett's SPCAT program by setting appropriate flags in the .int file to produce a .egy file. $P_{\rm mix}$ is the mixing coefficient for a given energy level when the effects of the coupling are included, and $(1-P_{\rm mix})$ indicates the degree to which a rotational energy level is affected by perturbation. The value of $(1-P_{\rm mix})$ ranges from zero to 0.5, where a value of zero indicates a pure state that is free from perturbation and a value of 0.5 indicates complete two-state mixing [30,31]. A list of the six largest values of $(1-P_{\rm mix})$ is given in Table 2. The rotational energy levels for the parent that have the highest calculated values are seen to be the 5_{14} ,0 $^+$ and 5_{15} ,0 $^-$ levels, each with a value of 0.484, indicating that they are heavily affected by perturbations.

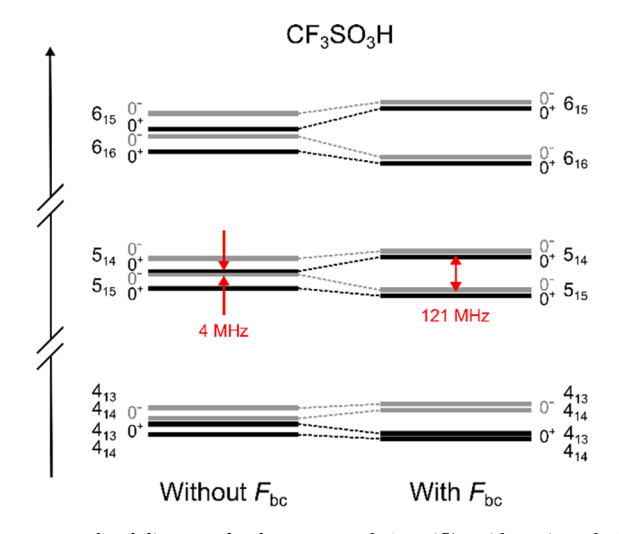
Spectra for the ³⁴S isotopologue were observed in natural abundance using both chirped-pulse and cavity spectrometers, and a pair of tunneling states was also identified. For $\mathrm{CF_3}^{34}\mathrm{SO_3H}$, 39 transitions were assigned to 36 frequencies, and included a-, b-, and c-type transitions from J''=1 up to J''=4 and up to $K_a{}''=2$. The separation between the ground and excited state transitions observed for $\mathrm{CF_3}^{34}\mathrm{SO_3H}$ were approximately the same as for the parent species, and b-type transitions were also found to cross tunneling states. Spectroscopic constants are included in Table 1. It is satisfying to note that for both the parent and ${}^{34}\mathrm{S}$ species, the fitted values of A, B, and C are virtually identical for the 0^+ and 0^- states.

Deuterated Triflic Acid: A pair of states was also observed in the

Table 2 Highly mixed rotational states for CF₃SO₃H and CF₃SO₃D.

CF ₃ SO ₃ H	$(1-P_{\mathrm{mix}})$	CF ₃ SO ₃ D ^a	$(1-P_{\rm mix})$
5 ₁₄ 0 ⁺	0.484398	$5_{32} F = 6 0^+$	0.470009
$5_{15}~0^-$	0.484398	$5_{33} F = 6 0^-$	0.470009
$6_{15}~0^{+}$	0.422553	$4_{31} F = 5 0^+$	0.298555
$6_{16}~0^-$	0.422552	$4_{32} F = 5 0^-$	0.298555
$4_{13} 0^+$	0.407339	$3_{30} F = 4 \ 0^+$	0.259695
$4_{14} \ 0^-$	0.407339	$3_{31} F = 4 \ 0^-$	0.259695

(a) F is the total angular momentum quantum number (corresponding to F = J + I, where I = 1 is the spin of the deuterium nucleus). The rotational states with largest F values have similar mixing coefficients to those shown for the levels of the same J, K_c , and tunneling state with smaller values of F. The energy levels with smaller values of F have been excluded for clarity.



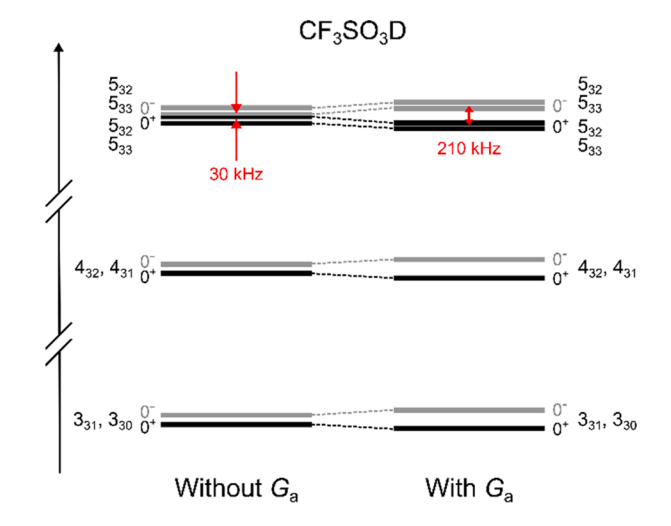


Fig. 5. Energy level diagrams for the parent and -OD triflic acid species calculated without and with a coupling constant. For visual clarity, only the rotational levels of the largest F for each J are shown in the -OD energy diagram. The rotational states shown for both species are the most highly mixed according to their respective calculated $(1 - P_{\text{mix}})$ values (see Table 2). For the parent species, a level crossing occurs at 5_{15} , 0^+ and 5_{14} , 0^- , which are separated by only about 4 MHz. For the -OD species, the 5_{32} , 0^+ and 5_{33} , 0^- F = 6 levels are nearly degenerate and separated by only about 30 kHz.

CF₃SO₃D spectra and the deuterium hyperfine structure for both ground and excited state transitions was resolvable with the cavity spectrometer. A total of 279 hyperfine components (103 rotational transitions) were measured and assigned for CF₃SO₃D from 3 to 18 GHz ranging from J'' = 0 up to J'' = 4 and up to $K_a'' = 4$. Compared with the parent and 34S species, the separation between the lower and upper state transitions for CF₃SO₃D is significantly decreased. Specifically, the separation of the pairs of states observed for the -OD species ranged only up to \sim 500 kHz, at most, compared with values of up to 154 MHz for the parent, as discussed above. The small splitting of the tunneling states initially presented a challenge in distinguishing the assignments for some ground and excited state transitions, particularly when combined with closely spaced K_a doublets of higher K_a transitions. But again, as for the parent species, closed loops proved instrumental. Unlike for the parent spectrum, however, a satisfactory fit could only be obtained by allowing the c-type transitions to cross between the tunneling states while assigning the b-type lines to transitions within each tunneling state. Indeed, despite extensive efforts for both isotopologues, the spectra could only be fit with b-type transitions crossing the tunneling doublet for the -OH form and c-type lines crossing between tunneling states for the -OD form. This reversal will be discussed further in the next section.

The CF_3SO_3D spectra were analyzed with the addition of a term, H_Q , added to Equation (1) for each tunneling state in order to treat the deuterium nuclear quadrupole coupling [32]. However, attempts to use an interaction Hamiltonian of the form given in Equation (2) resulted in highly correlated constants, and numerous attempts to include different combinations of F_{ab} , F_{bc} , and F_{ac} proved similarly unsuccessful. The form of H_{int} that was found to provide a satisfactory fit was

$$H_{int} = G_a P_a \tag{3}$$

Because the c-component of the dipole moment appears to be inverted for the -OD isotopologue (since the c-type transitions cross the tunneling doublet), the rotations about the a- and b-axes belong to the odd symmetry species A''. Thus, terms involving F_{bc} and F_{ac} would be able to connect the 0^+ and 0^- tunneling states. A successful fit was achieved, however, with only the G_aP_a term, which corresponds to an instantaneous principal axis formulation and is analogous to the F_{bc} term used to treat the parent in the reduced axis system [25,33]. The difference between the efficacy of the two treatments most likely arises from differences in the couplings that are most strongly manifested in the observed spectrum. (As seen in Fig. 5, near resonances in the -OD form occur for $K_a = 3$ states, whereas the near-degeneracies in the protonated form occur for $K_a = 1$ states.) The better success of G_xP_x terms compared with the $F_{yz}(J_yJ_z + J_zJ_y)$ type terms (x, y, z, = a, b or c) has been

previously noted in cases where the tunneling frequency is comparable to the asymmetry splittings [34,35], which is indeed the case for CF_3SO_3D . For example, the unperturbed asymmetry splitting of rotational energy levels J''=4 and $K_a{''}=3$ (4₃₂ and 4₃₁) is only about 30 kHz, which is even smaller than the value of ΔE (246 kHz).

The addition of the interaction term was much less important for the deuterated species than was the F_{bc} term for the protonated forms and indeed provided only a small improvement in the fit. The results of two fits for CF_3SO_3D with and without G_a are given in Table 3. Indeed, an acceptable fit for CF₃SO₃D was initially obtained for transitions involving only $K_a'' = 0$ and 1 using ΔE as an adjustable parameter, without having to include the coupling term. This fit produced a preliminary value for the tunneling energy of about 250 kHz, which is almost identical to the final value of 246 kHz appearing in Table 3 [36]. However, adding transitions involving $K_a \ge 2$ caused the fit to deteriorate and, although the G_a term was determinable and lowered the RMS value by a few kHz, Δ_K was found to provide the most significant benefit. The frequencies assigned to the $4_{32} \leftarrow 3_{21}$, $4_{31} \leftarrow 3_{21}$, $4_{32} \leftarrow 3_{22}$, and 4_{31} ← 3₂₂ quartet of transitions, which are included in the fits, could not be fit within the estimated experimental accuracy, with residuals in the 11-23 kHz range in Fit #2, and were the main contributors to the increased RMS. Attempts to expand G_a with J- and/or K-dependent distortion terms, as well as to include the other symmetry-allowed Coriolis coupling terms and their respective distortion terms, had little to no effect on the fit.

It is interesting to note that the fitted values of Δ_K for the 0^+ and 0^- states are of approximately equal magnitude but opposite sign, suggesting that they may be absorbing some additional untreated interaction. Nevertheless, the residuals are by no means egregiously large compared with the experimental uncertainties. The 4_{32} , 0^- and 4_{31} , 0^+ levels are among the rotational states for CF₃SO₃D that are highly mixed based on their $(1-P_{\rm mix})$ values (see Table 2). The largest values of $(1-P_{\rm mix})$ are calculated for 5_{33} , 0^- and 5_{32} , 0^+ states which are separated by only about 30 kHz, as indicated in the CF₃SO₃D energy level diagram of $K_a=3$ states from J=3-5 in Fig. 5. Although the coupling term for CF₃SO₃D is small, its inclusion was necessary to approximately simulate the relative intensities of the ground and excited state transitions. As with F_{bc} , the sign of G_a is not determinable, but the relative intensities of the pairs of 0^+ and 0^- transitions are better reproduced when the sign of the product G_a : μ_b : μ_c is negative.

4. Discussion

The predicted and fitted constants for triflic acid are compared in Table 4. Despite the presence of the hydroxyl large amplitude motion, it

Table 3 Spectroscopic constants from two combined fits of lower and upper states for deuterated triflic acid with and without the Coriolis coupling parameter G_{a} .

	Fit #1		Fit #2		
	0+	0-	0+	0-	
A [MHz]	2618.8990(10)	2618.6960(11)	2618.89472(64)	2618.70128(69)	
B [MHz]	1577.45954(37)	1577.45900(37)	1577.45906(20)	1577.45914(20)	
C [MHz]	1554.31449(43)	1554.31414(44)	1554.31439(22)	1554.31415(23)	
Δ_J [kHz]	0.142(10)	0.122(10)	0.1310(55)	0.1303(57)	
Δ_{JK} [kHz]	-0.019(45)	0.138(45)	0.094(27)	0.078(28)	
Δ_K [kHz]	11.38(11)	-11.43(11)	9.93(10)	-10.01(10)	
χ_{aa} [MHz]	-0.1240(67)	-0.1240(67)	-0.1317(38)	-0.1288(37)	
$\chi_{bb}\chi_{cc}$ [MHz]	0.167(12)	0.165(12)	0.1552(64)	0.1556(60)	
G _a [MHz] ^b			0.03575(67)		
ΔE [MHz]	0.2516(36)		0.2460(20)		
N^{c}	279		279		
RMS [kHz] ^d	10.2		5.4		

⁽a) Numbers in parentheses are one standard error in the least squares fit.

⁽b) Sign cannot be determined in the fit.

⁽c) Number of assigned hyperfine components, which includes 245 distinct frequencies and 103 rotational transitions.

⁽d) Root-mean square deviation of the residuals.

Table 4Comparison of theoretical and experimental values for the triflic acid isotopologues. ^a

	M06-2X/6-311++G(3df,3pd)			Experimental ^b		
	Parent	CF ₃ ³⁴ SO ₃ H	CF ₃ SO ₃ D	Parent	CF ₃ ³⁴ SO ₃ H	CF ₃ SO ₃ D ^c
A [MHz]	2683.0	2682.6	2631.3	2669.06754(18)	2668.69479(39)	2618.89472(64)
B [MHz]	1599.5	1591.5	1588.0	1586.31446(17)	1578.45686(30)	1577.45906(20)
C [MHz]	1589.0	1581.2	1563.4	1582.53271(12)	1574.85992(33)	1554.31439(22)
χ_{aa} [MHz]			-0.152			$-0.1317(38)^{d}$
χ_{bb} - χ_{cc} [MHz]			0.184			0.1552(64) ^d
ΔA [MHz]		-0.4	-51.7		-0.4	-50.2
ΔB [MHz]		-8.0	-11.5		-7.9	-8.9
ΔC [MHz]		-7.8	-25.6		-7.7	-28.2
$ \mu_a $ [D] ^e	0.5	0.5	0.4	≠0	≠0	≠0
$ \mu_b $ [D] ^e	2.5	2.5	2.8	≠0	≠ 0	≠0
$ \mu_c $ [D] ^e	1.3	1.3	0.4	≠ 0	≠ 0	≠ 0

- (a) Isotope shifts are the values of the isotopologue rotational constants minus those of the parent rotational constants.
- (b) Fitted constants and the resulting isotope shifts for the lower state (0^+) are shown. The observed isotope shifts using the fitted constants for the upper state values are the same to within a few kHz except for the value ΔA for CF₃SO₃D, which is -50.4 MHz using the upper state values.
- (c) Fitted constants from Fit #2 for CF₃SO₃D are shown here and were used to calculate the isotope shift. The values of the isotope shifts using the constants from Fit #1 are the same as those shown in the table.
- (d) The upper state values of χ_{aa} and χ_{bb} - χ_{cc} obtained for CF₃SO₃D from Fit #2 are -0.1288(37) MHz and 0.1556(60) MHz, respectively.
- (e) The " \neq 0" entries in the experimental columns arise from the observation of a-, b-, and c-type transitions.

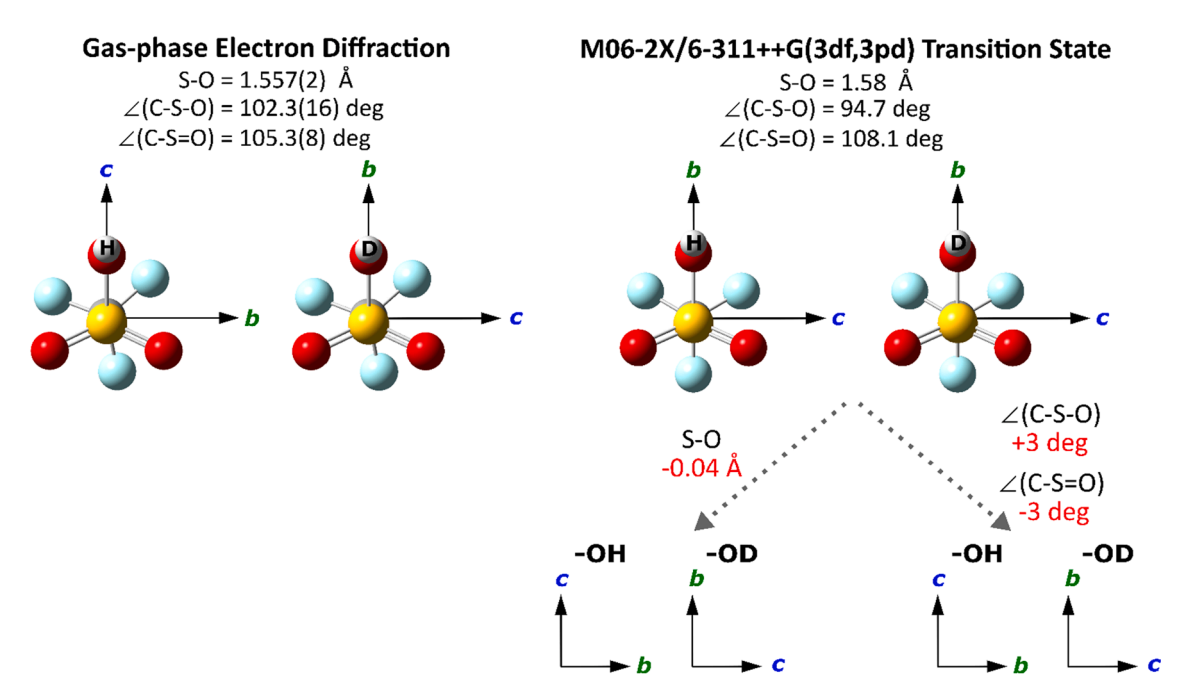


Fig. 6. Triflic acid structure reported from gas-phase electron diffraction (left, Ref [11]) and transition state structure calculated at the M06-2X/6-311++G(3df,3pd) level of theory (right). Both the -OH and -OD isotopologues are shown in their respective principal axis systems. The values of the S-O bond length as well as the C-S-O and C-S=O angles are also shown. The orientation of the principal axis systems for -OH and -OD is also shown for the predicted transition state structure when the S-O bond is decreased by 0.04 Å and when both the C-S-O and C-S=O angles are changed (increase of 3 degrees for C-S-O and decrease of 3 degrees for C-S-O and C-S-O a

can be seen that the experimental constants are in good agreement (within 0.8%) of those calculated from the theoretical equilibrium structure. Additionally, the observation of a-, b-, and c-type transitions for all isotopologues is consistent with the prediction of non-vanishing dipole moment components on all three inertial axes and precludes the possibility of having observed a vibrationally averaged structure of C_s symmetry for which one of the vibrationally averaged dipole moment components would vanish. The shifts in the rotational constants upon isotopic substitution are also given in Table 4 and, while the observed 34 S shifts are in excellent agreement with the predicted values, there are slight discrepancies of up to 2.6 MHz for CF₃SO₃D. This likely arises because of (i) differences in vibrational averaging of the -OH and -OD moieties and (ii) the larger magnitude of the shifts which amplifies discrepancies due to the calculated structures. Overall, however, the

errors in the isotope shifts are sufficiently small as to cause no concern.

It is of interest to compare the present results with those previously obtained from gas phase electron diffraction [11]. The reported structure from that work is shown in Fig. 6. Although this remains the best experimental structure to date, the C-S-O-H dihedral angle could not be determined and was fixed to 180 degrees for the analysis. This value not only differs significantly from the 92 degrees predicted here for the minimum energy structure but also corresponds to a transition state structure, rather than an energy minimum (Fig. 2). The derived rotational constants and Cartesian coordinates from the reported structure are provided in the Supplementary Material.

An unexpected result from this study is the observation that b-type transitions cross between tunneling states in the -OH species while c-type transitions do so in the -OD species. In this regard, it is significant

Table 5Comparison of the tunneling energies determined for -OH and -OD species of various molecules. ^a

	$\Delta E(\text{-OH})/\Delta E(\text{-OD})$	ΔE (-OH) [MHz]	$\Delta E(\text{-OD})$ [MHz]	Barrier height [cm ⁻¹] ^h
Triflic acid ^b	215	52.96784(65)	0.2460(20)	980
4-chlorophenol ^c	211	79.496(11)	0.376(3)	1148
4-fluorophenol ^c	152	177.121(8)	1.165(6)	1006
2,2,2-trifluoroethanol ^d	28	5868.6952(16)	208.5037(43)	763
Cyclopropanol ^e	25	4115.26(42)	163.7(18)	660
Benzyl alcohol ^f	4	492.816(2)	136.306(4)	280
Propargyl alcohol ^g	3	652389.42(21)	213480(31)	90

- (a) The tunneling path for the molecules listed here is an internal rotation of the -OH or -OD hydroxyl group. Systems with significant V_2 and V_3 barriers are not included.
- (b) This work.
- (c) Reference [39].
- (d) Reference [40], gauche conformer.
- (e) Reference [41], gauche conformer.
- (f) Reference [42].
- (g) References [43,44], gauche conformer.
- (h) In the few cases where the barrier was separately determined and reported for both the -OH and -OD species, only the value of the barrier for -OH is listed.

to note that in the absence of the hydrogen, the molecule is a symmetric top and the orientation of the b- and c-axes is ill-defined. The presence of the hydrogen pins the location of the axes but the value of (B-C) is very small (only 3.8 MHz for the parent species). To determine which transition types cross the tunneling doublet, the dipole matrix elements can be factored as follows:

$$\langle 0^{-}, J_{\tau}^{'} | \mu_{g}(Q) \cos \theta_{gZ} | 0^{+}, J_{\tau}^{"} \rangle = \langle 0^{-} | \mu_{g}(Q) | 0^{+} \rangle \langle J_{\tau}^{'} | \cos \theta_{gZ} | J_{\tau}^{"} \rangle \tag{4}$$

where Q represents the tunneling coordinate. Note that for triflic acid, the inertial axes rotate as the OH bond vector proceeds along the tunneling coordinate. Thus, the most straightforward application of symmetry arguments to evaluate $\langle 0^-|\mu_g(Q)|0^+\rangle$ involves consideration of the symmetry of $\mu_g(Q)$ in the same coordinate system in which $|0^+\rangle$ and $\langle 0^-|$ have definite symmetry, i.e., the inertial axis system of the C_s transition state structure. This is the coordinate system of the symmetric double-well potential and hence of the one that defines "left" and "right" states whose linear combinations form the 0^+ and 0^- tunneling states. The current situation differs from other problems in which the inertial axis system of the transition state coincides with that of either equilibrium structure, thus allowing the selection rules to be determined simply by inspecting the directions of dipole moment components in the two potential energy minima.

At the calculated transition state structure for both the -OH and -OD species, the *c*-axis is oriented such that the tunneling motion inverts μ_c (i. e., $\mu_c = 0$ at the transition state). This is consistent with the observed spectrum for the -OD species but not the parent, suggesting the possibility that the orientation of the b- and c-axes differs between the two isotopologues [37]. While this does not appear to be the case at either the calculated equilibrium or transition state structures, it can be shown that the axis definitions are, in fact, very sensitive to small changes in the structure. For example, using the structure determined from electron diffraction (with the C-S-O-H angle of 180 degrees, equivalent to the transition state geometry), we find that $\mu_b = 0$ for both the parent and $^{34}\mathrm{S}$ species while μ_c becomes zero for the -OD species. Moreover, looking specifically at individual structural parameters of the theoretical structure, if the S-O bond length is decreased by only 0.04 Å from 1.58 Å to 1.54 Å the same axis definitions in the minimum energy structures for -OH and -OD is maintained, but the transition state structure for -OH becomes symmetric in the ac-plane ($\mu_b=0$) while the -OD transition state structure stays symmetric in the ab-plane ($\mu_c = 0$). This result of different planes of symmetry in the -OH and -OD transition state structures can also be obtained by increasing the C-S-O angle by only 3 degrees (from 94.7 to 97.7 degrees) while decreasing the C-S=O angles by the same amount (from 108 to 105 degrees). A summary of the effects of these changes on the orientation of the axis systems in the -OH and -OD

transition states is shown in Fig. 6. In light of these results, it seems plausible that the combination of even smaller deviations from the predicted equilibrium structures in both these structural parameters as well as those not tested (and/or differences in vibrational averaging between the parent and deuterated forms), could lead to the different axis orientations in the vibrationally averaged transition state structures and hence the isotopic dependence of the selection rules. Such a situation would be quite unusual, but likely arises in this case because the molecule is so nearly a symmetric top.

Finally, it is apparent from Tables 1 and 3 that the tunneling splitting, ΔE , is highly sensitive to deuteration, with a value of ΔE (-OH)/ ΔE (-OD) equal to 215. While this ratio is large, however, it is not unprecedented. Table 5 compares several systems in the literature exhibiting a simple, 1-dimensional hydroxyl tunneling motion in which tunneling splittings for both the -OH and -OD species were determined. A similar comparison of -OH and -OD tunneling energies and a correlation between them have been recently noted [38]. Here, it can be seen that the $\Delta E(\text{-OH})/\Delta E(\text{-OD})$ ratio for triflic acid is the largest among the systems listed, but comparable to that of 4-chlorophenol and only slightly larger than that of 4-fluorophenol [39]. Also listed in the table are the barriers to inversion, and it may be seen that there is a reasonable correlation between $\Delta E(\text{-OH})/\Delta E(\text{-OD})$ and the barrier height. Thus, the observed ratio and the calculated barrier of height of 2.8 kcal/mol (980 cm⁻¹) for triflic acid are fully consistent with the trend. Interestingly, the molecules with a larger barrier and $\Delta E(\text{-OH})/\Delta E(\text{-OD})$ are those with electron-withdrawing substituents.

5. Conclusion

The microwave spectra for CF₃SO₃H, CF₃³⁴SO₃H, and CF₃SO₃D have been recorded and assigned. As a result of large amplitude motion of the hydroxyl group rotating about the S-O bond, a pair of tunneling states was observed in the spectra for each isotopologue. The lowest barrier height to this motion was calculated to be 2.8 kcal/mol at the M06-2X/6-311++G(3df,3pd) level of theory and occurs at the transition state when the C-S-O-H dihedral angle is 180 degrees (OH pointing away from the CF₃ group). The tunneling energy, ΔE , was determined to be 52.96784(65) MHz and 52.8761(16) MHz for CF₃SO₃H and CF₃³⁴SO₃H, respectively, and upon deuteration decreased significantly to 0.2460(20) MHz. Additionally, the rotational transition type that crossed tunneling states changed from -OH to -OD, with b-type transitions crossing the tunneling doublet in the -OH species and c-type transitions crossing in the -OD species. This could be a result of axis switching at the transition state structure from -OH to -OD assuming the possibility of errors in the calculated structure and/or slight deviations of the experimental structure from the predicted equilibrium structures due to the effects of vibrational averaging.

CRediT authorship contribution statement

Anna K. Huff: Investigation, Validation, Formal analysis, Writing – original draft, Writing – review & editing. **Nathan Love:** Investigation, Writing – review & editing. **C.J. Smith:** Investigation. **Kenneth R. Leopold:** Supervision, Resources, Project administration, Writing – review & editing.

Declaration of Competing Interest

The authors declare that they have no known competing financial interests or personal relationships that could have appeared to influence the work reported in this paper.

Acknowledgments

This work was supported by the National Science Foundation (Grant No. CHE–1953528) and the Minnesota Supercomputing Institute. The authors are grateful to Professors Peter Groner, Mark Marshall, Helen Leung, and Zbigniew Kisiel for valuable input on various aspects of this work.

Appendix A. Supplementary material

Calculated O9-S1-O2-H3 dihedral angle and -OH torsion barrier height from different levels of theory; Tables of transition frequencies, assignments, and residuals from the least squares fits for all isotopologues studied; Theoretical Cartesian coordinates for the minimum energy and transition state structures; Derived rotational constants and Cartesian coordinates of the structure reported from gas-phase electron diffraction. Supplementary data to this article can be found online at htt ps://doi.org/10.1016/j.jms.2022.111623.

References

- [1] G.A. Olah, G.K.S. Prakash, J. Sommer, Superacids, Science 206 (4414) (1979) 13–20, https://doi.org/10.1126/science.206.4414.13.
- [2] R.D. Howells, J.D. Mc Cown, Trifluoromethanesulfonic Acid and Derivatives, Chem. Rev. 77 (1977) 69–92, https://doi.org/10.1021/cr60305a005.
- [3] A.N. Kazakova, A.V. Vasilyev, Trifluoromethanesulfonic Acid in Organic Synthesis, Russ. J. Org. Chem. 53 (2017) 485–509, https://doi.org/10.1134/ \$1077429017040017
- [4] T. Ishimoto, T. Ogura, M. Koyama, Stability and hydration of model perfluorosulfonic acid compound systems, CF₃SO₃H (H₂O)_n (n = 1-4) and its isotopomer by the direct treatment of H/D nuclear quantum effects, Comput. Theor. Chem. 975 (2011) 92–98, https://doi.org/10.1016/j.comptc.2011.02.006.
- [5] K. Sagarik, M. Phonyiem, C. Lao-Ngam, S. Chaiwongwattana, Mechanisms of proton transfer in Nafion®: Elementary reactions at the sulfonic acid groups, PCCP 10 (2008) 2098–2112, https://doi.org/10.1039/b718480h.
- [6] C. Wang, J.K. Clark II, M. Kumar, S.J. Paddison, An ab initio study of the primary hydration and proton transfer of CF₃SO₃H and CF₃O(CF₂)₂SO₃H: Effects of the hybrid functional and inclusion of diffuse functions, Solid State Ionics 199–200 (2011) 6–13, https://doi.org/10.1016/j.ssi.2011.07.002.
- [7] I. Kendrick, A. Yakaboski, E. Kingston, J. Doan, N. Dimakis, E.S. Smotkin, Theoretical and experimental infrared spectra of hydrated and dehydrated nafion, J. Polym. Sci., Part B: Polym. Phys. 51 (2013) 1329–1334, https://doi.org/ 10.1002/polb.23348.
- [8] C. Wakai, T. Shimoaka, T. Hasegawa, Analysis of the hydration process and rotational dynamics of water in a Nafion membrane studied by ¹H NMR spectroscopy, Anal. Chem. 85 (2013) 7581–7587, https://doi.org/10.1021/ ac401653y
- [9] R.K. Singh, K. Kunimatsu, K. Miyatake, T. Tsuneda, Experimental and Theoretical Infrared Spectroscopic Study on Hydrated Nafion Membrane, Macromolecules 49 (2016) 6621–6629. https://doi.org/10.1021/acs.macromol.6b00999.
- [10] F. Sepehr, S.J. Paddison, Primary hydration and proton transfer of electrolyte acids: An ab initio study, Solid State Ionics 306 (2017) 2–12, https://doi.org/ 10.1016/j.ssi.2017.03.013.
- [11] G. Schultz, I. Hargittai, R. Seip, Electron diffraction investigation of the molecular structure of trifluoromethanesulphonic acid (triflic acid), Z. Naturforsch. A 36 (1981) 917–918.
- [12] Y. Katsuhara, R.M. Hammaker, D. DesMarteau, Synthesis and Properties of Chlorine(I) and Bromine(I) Trifluoromethanesulfonates and Raman Spectra of

- CF₃SO₂X (X = F, OH, OC1), Inorg. Chem. 19 (1980) 607–616, https://doi.org/10.1021/ic50205a007.
- [13] E.L. Varetti, The infrared spectra of trifluoromethanesulphonic acid in different states of aggregation, Spectrochim. Acta A 44 (1988) 733.
- [14] H.G.M. Edwards, The vibrational spectrum of trifluoromethanesulphonic acid, CF₃SO₃H, and the determination of its degrees of dissociation in aqueous solution by Raman spectroscopy, Spectrochim. Acta A 45 (1989) 715–719, https://doi.org/ 10.1016/0584.8539(80)80257-0
- [15] J.R. Lane, H.G. Kjaergaard, K.L. Plath, V. Vaida, Overtone spectroscopy of sulfonic acid derivatives, J. Phys. Chem. A 111 (2007) 5434–5440, https://doi.org/ 10.1021/jp0688005.
- [16] N. Love, A.K. Huff, K.R. Leopold, Proton transfer in a bare superacid-amine complex: A microwave and computational study of trimethylammonium triflate, J. Phys. Chem. A 125 (23) (2021) 5061–5068.
- [17] A.K. Huff, N. Love, K.R. Leopold, Microwave study of triflic acid hydrates: Evidence for the transition from hydrogen-bonded clusters to a microsolvated ion pair, J. Phys. Chem. A 125 (2021) 8033–8046, https://doi.org/10.1021/acs. jpca.1c06815.
- [18] M.J. Frisch, G.W, Trucks, H.B. Schlegel, G.E. Scuseria, M.A. Robb, J.R. Cheeseman, G. Scalmani, V. Barone, G.A. Petersson, X.L. Nakatsuji, et al. Gaussian 16; Gaussian, Inc.: Wallingford, CT, 2016.
- [19] B.P. Pritchard, D. Altarawy, B. Didier, T.D. Gibson, T.L. Windus, A New Basis Set Exchange: An Open, Up-to-date Resource for the Molecular Sciences Community, J. Chem. Inf. Model. 59 (2019) 4814–4820, https://doi.org/10.1021/acs. icim.0b00795
- [20] J.A. Phillips, M. Canagaratna, H. Goodfriend, A. Grushow, J. Almlöf, K.R. Leopold, Microwave and ab initio investigation of HF-BF₃, J. Am. Chem. Soc. 117 (1995) 12549–12556, https://doi.org/10.1021/ja00155a018.
- [21] C.T. Dewberry, R.B. Mackenzie, S. Green, K.R. Leopold, 3D-printed slit nozzles for Fourier transform microwave spectroscopy, Rev. Sci. Instrum. 86 (2015) 065107-1–7. https://doi.org/10.1063/1.4922852.
- [22] M. Canagaratna, J.A. Phillips, H. Goodfriend, K.R. Leopold, Structure and bonding of the sulfamic acid zwitterion: microwave spectrum of ⁺H₃N-SO₃, J. Am. Chem. Soc. 118 (1996) 5290–5295.
- [23] H.M. Pickett, The fitting and prediction of vibration-rotation spectra with spin interactions, J. Mol. Spectrosc. 148 (1991) 371–377, https://doi.org/10.1016/ 0022-2852(91)90393-O.
- [24] J.K.G. Watson, Aspects of Quartic and Sextic Centrifugal Effects on Rotational Energy Levels, in J.R. Durig (Ed.) Vibrational Spectra and Structure, Elsevier Scientific Publishing, Amsterdam, 1977, pp. 1–89.
- [25] H.M. Pickett, Vibration-rotation interactions and the choice of rotating axes for polyatomic molecules, J. Chem. Phys. 56 (1972) 1715–1723, https://doi.org/ 10.1063/1.1677430.
- [26] I.M. Mills, Coriolis interactions, intensity perturbations and potential functions in polyatomic molecules, Pure Appl. Chem. 11 (1965) 325, https://doi.org/10.1351/ pac196511030325.
- [27] W.G. Read, E.A. Cohen, H.M. Pickett, The rotation-inversion spectrum of cyanamide, J. Mol. Spectrosc. 115 (1986) 316–332, https://doi.org/10.1016/ 0022-2852(86)90050-0.
- [28] R.D. Suenram, F.J. Lovas, H.M. Pickett, The Microwave Spectrum and Molecular Conformation of Peroxynitric Acid (HOONO₂), J. Mol. Spectrosc. 116 (1986) 406–421, https://doi.org/10.1016/0022-2852(86)90136-0.
- [29] D. Christen, H.S.P. Müller, The millimeter wave spectrum of aGg' ethylene glycol: The quest for higher precision, PCCP 5 (2003) 3600–3605, https://doi.org/ 10.1039/b304566h.
- [30] R.A.H. Butler, D.T. Petkie, P. Helminger, F.C. De Lucia, Z. Kisiel, The rotational spectrum of chlorine nitrate (ClONO₂): The v₅/v₆v₉ dyad, J. Mol. Spectrosc. 243 (2007) 1–9, https://doi.org/10.1016/j.jms.2007.02.023.
- [31] Z. Kisiel, L. Pszczółkowski, B.J. Drouin, C.S. Brauer, S. Yu, J.C. Pearson, I. R. Medvedev, S. Fortman, C. Neese, Broadband rotational spectroscopy of acrylonitrile: Vibrational energies from perturbations, J. Mol. Spectrosc. 280 (2012) 134–144, https://doi.org/10.1016/j.jms.2012.06.013.
- [32] W. Gordy, R.L. Cook, Microwave Molecular Spectra, third ed., John Wiley and Sons, New York, 1984.
- [33] D.O. Harris, H.W. Harrington, A.C. Luntz, W.D. Gwinn, Microwave spectrum, vibration-rotation interaction, and potential function for the ring-puckering vibration of trimethylene sulfide, J. Chem. Phys. 44 (1966) 3467–3480, https:// doi.org/10.1063/1.1727251.
- [34] J.C. López, J.L. Alonso, F.J. Lorenzo, V.M. Rayón, J.A. Sordo, The tetrahydrofuran...hydrogen chloride complex: Rotational spectrum and theoretical analysis, J. Chem. Phys. 111 (1999) 6363–6374, https://doi.org/ 10.1063/1.479962.
- [35] J.C. Lopez, J.L. Alonso, R. Cervellati, A. Degli Esposti, D.G. Lister, P. Palmieri, Conformation and ring inversion in γ-butyrolacetone Part 1. Microwave spectrum, J. Chem. Soc. Farad. Trans. 86 (1990) 453–458.
- [36] It is reassuring that the fit using F_{bc} instead of G_a , returned a very similar value of 261.3(31) kHz for the tunneling splitting, despite the high correlation among fitted constants.
- [37] The possibility of ambiguous state labeling due to strong mixing was also considered. However, inspection of the calculated energies of the most perturbed levels of the protonated species as a function of F_{bc} did not reveal any abrupt changes in labeling.
- [38] R. Medel, Simple models for the quick estimation of ground state hydrogen tunneling splittings in alcohols and other compounds, Phys. Chem. Chem. Phys. 23 (2021) 17591–17605, https://doi.org/10.1039/D1CP02115J.

- [39] N.W. Larsen, Microwave spectra and internal rotation of 4-fluorophenol, 4chlorophenol and 4-bromophenol, J. Mol. Struct. 144 (1986) 83–99, https://doi. org/10.1016/0022-2860(86)80169-7.
- [40] L.-H. Xu, G.T. Fraser, F.J. Lovas, R.D. Suenram, C.W. Gillies, H.E. Warner, J. Z. Gillies, The microwave spectrum and OH internal rotation dynamics of gauche-2,2,2-trifluoroethanol, J. Chem. Phys. 103 (1995) 9541–9548, https://doi.org/10.1063/1.469068
- [41] J.N. MacDonald, D. Norbury, J. Sheridan, Microwave spectrum, dipole moment and internal rotation function of gauche-cyclopropanol, J. Chem. Soc. Faraday
- Trans. 2 Mol Chem. Phys. 74 (1978) 1365–1375, https://doi.org/10.1039/F29787401365
- [42] K.A. Utzat, R.K. Bohn, J.A. Montgomery Jr., H.H. Michels, W. Caminati, Rotational spectrum, tunneling motions, and potential barriers of benzyl alcohol, J. Phys. Chem. A 114 (2010) 6913–6916.
- [43] J.C. Pearson, B.J. Drouin, The ground state torsion-rotational spectrum of propargyl alcohol (HCCCH₂OH), J. Mol. Spectrosc. 234 (2005) 149–156, https://doi.org/10.1016/j.jms.2005.08.013.
- [44] E. Hirota, Internal rotation in propargyl alcohol from microwave spectrum, J. Mol. Spectrosc. 26 (1968) 335–350, https://doi.org/10.1016/0022-2852(68)90069-6.